


Dual to the anomalous weak-value effect of photon-polarization separationJames Q. Quach **Institute for Photonics and Advanced Sensing and School of Chemistry and Physics, The University of Adelaide, South Australia 5005, Australia*

(Received 25 March 2019; published 22 November 2019)

The quantum Cheshire cat (QCC) thought experiment proposes that a quantum object's property (e.g., polarization, spin, etc.) can be separated from its physical body. This conclusion arose from an argument that interprets a zero weak value (WV) of polarization as no polarization. We show that this argument is incomplete in the sense that a zero WV reading could equally be interpreted as linear polarization. Nevertheless, through a generalization of the QCC, we complete their argument by excluding the possibility of linear polarization as a consistent interpretation. We go further and introduce the dual of the generalized QCC. The dual QCC exhibits an intriguing effect, where a horizontally polarized interferometer with just one arm can give rise to interference which is vertically polarized. The interference appears to arise as the result of the phase difference between the physical arm and a *phantom* arm. This peculiar effect arises from the interplay between the preselected and postselected states, which characterize WVs. The QCC has not yet been unambiguously experimentally demonstrated. The QCC dual offers an alternative pathway to experimental realization.

DOI: [10.1103/PhysRevA.100.052117](https://doi.org/10.1103/PhysRevA.100.052117)**I. INTRODUCTION**

The conventional view of measurement in quantum mechanics is that it is a destructive process that irrevocably projects the system into an eigenstate of the observed variable. *Weak measurements* provide a formal nondestructive measurement scheme by weakly coupling the system to an ancilla and performing a measurement (projection) on the ancilla in some appropriate basis [1–5]. Operationally, the ancilla is a measurement device with a pointer; the interaction of the system and the ancilla shifts the pointer state proportional to the magnitude of the observed variable. As the ancilla interacts only very weakly with the system, the state can evolve without appreciable disturbance.

Weak values seek to represent the observables of intermediate states, as the system evolves from a preselection to a postselection state. It is a unique consequence of quantum mechanics that one may choose both preselection *and* postselection states, which distinguishes it from classical mechanics, where the choice of the initial state defines the final state, or vice versa. This idea is more generally explored in the two-state vector formalism [6]. By judicious postselection, weak values (WVs) have been used to amplify small signals [7–24], provide direct determination of quantum states and geometric phases via the complex nature of WVs [25–32], and give conditioned averages associated with observables [33–35]. In an intriguing proposal Aharonov *et al.* [1] showed that WVs can give rise to a situation where the position of a photon exists in one arm of an interferometer while its polarization exists in the other arm. The effect was given the name quantum Cheshire cat, which alludes to Lewis Carroll's

Cheshire cat, whose grin (polarization) could exist without its body (photon).

The search for dualities has been a fruitful path to insights and novel phenomena in physics, e.g., the wave-particle duality, electromagnetic duality, the Aharonov-Casher effect [36] and its dual [37,38], and many more. Here we first generalize the quantum Cheshire cat (QCC) with elliptical polarizations, and then we introduce the dual of the QCC and discuss its behavior. There has been a discussion on the physical interpretation of WVs since its inception (see [39–43] and references therein). We take the approach that a WV represents a physical property of the quantum system being measured, in the same spirit as the original QCC.

II. WEAK VALUES

If we precisely know the position of a quantum particle, we have no information about its speed. However, we may place weak detectors all around the particle to deduce its average speed by measuring the time it took to reach the detectors. We may also ask, What is the speed of the particle to reach a subset of locations as detected by a subensemble of the detectors? The answer to this question is a WV.

Prior to measurement the preselected state $|\psi_i\rangle$ and pointer state $|m_i\rangle$ are uncoupled. In the weak measurement scheme, the interaction Hamiltonian between the system and pointer is

$$\hat{H}_{\text{int}} = g(t)\hat{O}\hat{P}, \quad (1)$$

which couples the system's observable \hat{O} to the pointer momentum \hat{P} . The interaction with the pointer occurs for a short time, outside of which the coupling constant g is zero, so that the evolutionary operator is $\hat{U} = \exp(-\frac{i}{\hbar} \int \hat{H}_{\text{int}} dt) = \exp(-\frac{i}{\hbar} g \hat{O} \hat{P})$. After the interaction with the pointer, the system undergoes a projective measurement where only a subset of the measured states are chosen. Labeling this postselected

*quach.james@gmail.com

state $|\psi_f\rangle$, the final pointer state is ($\hbar = 1$)

$$\begin{aligned} |m_f\rangle &= \langle\psi_f|\exp(-ig\hat{O}\hat{P})|\psi_i\rangle|m_i\rangle \\ &\approx \langle\psi_f|\psi_i\rangle\left(1 - ig\frac{\langle\psi_f|\hat{O}|\psi_i\rangle}{\langle\psi_f|\psi_i\rangle}\hat{P}\right)|m_i\rangle \\ &\approx \langle\psi_f|\psi_i\rangle\exp(-ig\langle\hat{O}\rangle_w\hat{P})|m_i\rangle, \end{aligned} \quad (2)$$

where

$$\langle\hat{O}\rangle_w \equiv \frac{\langle\psi_f|\hat{O}|\psi_i\rangle}{\langle\psi_f|\psi_i\rangle} \quad (3)$$

is known as the WV of \hat{O} .

The pointer momentum \hat{P} is conjugate to the pointer position \hat{X} . Let us now write the initial pointer state in the position basis, $|m_i\rangle = \int dx|x\rangle\varphi(x)$, where $\varphi(x) \equiv \langle x|m_i\rangle$ and is assumed to be real. The final pointer state in the position basis then is

$$\begin{aligned} |m_f\rangle &\approx \langle\psi_f|\psi_i\rangle\exp(-ig\langle\hat{O}\rangle_w\hat{P})\int dx|x\rangle\varphi(x) \\ &= \langle\psi_f|\psi_i\rangle\int dx|x\rangle\varphi(x - g\langle\hat{O}\rangle_w), \end{aligned} \quad (4)$$

where we have used the fact that \hat{P} acts as a translation operator that shifts the pointer state in the conjugate x basis by $g\langle\hat{O}\rangle_w$. If the pointer states were the positions of a needle on a measuring device, the interaction of the measurement device with the system will shift the position of the needle by a distance proportional to $\langle\hat{O}\rangle_w$, thereby giving us a measurement of observable \hat{O} .

III. GENERALIZED QUANTUM CHESHIRE CAT

The QCC is an interferometer experiment with preselection, postselection, and weak detectors. We generalize the preselection state of the QCC with a phase differential between the arms of the interferometer,

$$|\Phi_i\rangle = (e^{i\theta}|A\rangle + |B\rangle)|H\rangle/\sqrt{2}, \quad (5)$$

where $|A\rangle(|B\rangle)$ represents a state located in arm A (B) of the interferometer, and $|H\rangle(|V\rangle)$ is horizontal (vertical) polarization. The phase differential can be implemented with a phase shifter (PS1) in one of the arms as shown in Fig. 1. The original QCC preselection state is a special case of Eq. (5), where $\theta = \pi/2$.

The QCC postselection state is

$$|\Phi_f\rangle = (|A\rangle|H\rangle + |B\rangle|V\rangle)/\sqrt{2}. \quad (6)$$

The projectors in the QCC experiment measure the presence of photons in arms A and B,

$$\hat{A} = |A\rangle\langle A|(|L\rangle\langle L| + |R\rangle\langle R|), \quad (7)$$

$$\hat{B} = |B\rangle\langle B|(|L\rangle\langle L| + |R\rangle\langle R|), \quad (8)$$

and the polarization in arms A and B,

$$\hat{\sigma}_A = |A\rangle\langle A|(|L\rangle\langle L| - |R\rangle\langle R|), \quad (9)$$

$$\hat{\sigma}_B = |B\rangle\langle B|(|L\rangle\langle L| - |R\rangle\langle R|), \quad (10)$$

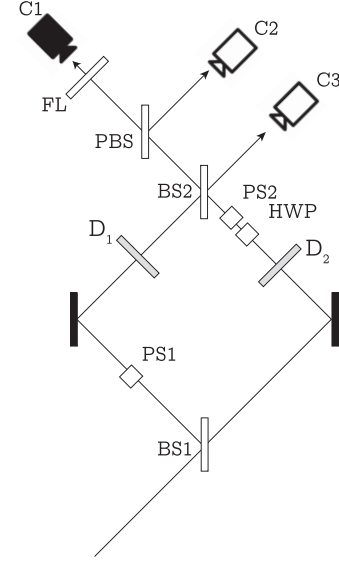


FIG. 1. A schematic of the generalized QCC, where a phase shifter (PS1) introduces a controllable phase difference $e^{i\theta}$ between the two arms. A half-wave plate (HWP), phase shifter (PS2), beam splitter (BS2), and polarizing beam splitter (PBS) are used for postselection. To project the pointer onto the momentum basis, a Fourier lens (FL) is used to Fourier transform the light beam so that each pixel on the camera corresponds to a transverse momentum. To project the pointer onto the position basis, remove the FL, and each pixel corresponds to a transverse displacement. Detectors $\hat{\sigma}_A$ and \hat{A} are placed at location D_1 , and $\hat{\sigma}_B$ and \hat{B} at location D_2 .

where

$$|L\rangle \equiv (|H\rangle + e^{i\phi}|V\rangle)/\sqrt{2}, \quad (11)$$

$$|R\rangle \equiv (|H\rangle - e^{i\phi}|V\rangle)/\sqrt{2} \quad (12)$$

are left-elliptical and right-elliptical polarization states. In comparison to the original QCC experiment, we have generalized the basis states to elliptical polarization states with the phase parameter ϕ . The original QCC circular-polarization basis is a special case of Eqs. (11) and (12), where $\phi = \pi/2$.

\hat{A} (\hat{B}) detects whether there is a photon in arm A (B). $\hat{\sigma}_A$ detects the polarization of the photon in arm A. The eigenvalues 1 and -1 correspond to eigenstates $|L\rangle|A\rangle \equiv |L, A\rangle$ and $|R, A\rangle$, which are states of left-elliptical and right-elliptical polarized photons in arm A, respectively, whereas the eigenvalue 0 corresponds to the degenerate subspace spanned by eigenstates $|L, B\rangle$ and $|R, B\rangle$, which are states of photons in arm B. $\hat{\sigma}_B$ is similarly defined.

Using Eq. (3), the WVs measured by these operators are

$$\langle\hat{A}\rangle_w = \langle\hat{A}\hat{L}\rangle_w + \langle\hat{A}\hat{R}\rangle_w = 1, \quad (13)$$

$$\langle\hat{B}\rangle_w = \langle\hat{B}\hat{L}\rangle_w + \langle\hat{B}\hat{R}\rangle_w = 0, \quad (14)$$

and

$$\langle\hat{\sigma}_A\rangle_w = \langle\hat{A}\hat{L}\rangle_w - \langle\hat{A}\hat{R}\rangle_w = 0, \quad (15)$$

$$\langle\hat{\sigma}_B\rangle_w = \langle\hat{B}\hat{L}\rangle_w - \langle\hat{B}\hat{R}\rangle_w = e^{i(\phi-\theta)}, \quad (16)$$

where

$$\hat{L} = |L\rangle\langle L|(|A\rangle\langle A| + |B\rangle\langle B|), \quad (17)$$

$$\hat{R} = |R\rangle\langle R|(|A\rangle\langle A| + |B\rangle\langle B|). \quad (18)$$

Note that $\langle \hat{A}\hat{L} \rangle_w = \langle \hat{A}\hat{R} \rangle_w = 1/2$ and $\langle \hat{B}\hat{L} \rangle_w = -\langle \hat{B}\hat{R} \rangle_w = e^{i(\phi-\theta)}/2$. For $\theta = \phi = \pi/2$ we retrieve the original QCC result, which the QCC authors interpret as the photon existing in arm A while its left-circular polarization is detected in arm B. The generalized QCC generalizes this to the detection of elliptical polarization in arm B. It shows that the polarization is determined by the phase difference between the interferometer arms. Specifically, let us rotate the polarization basis of $\hat{\sigma}_B$ so that $\phi = \theta$. In this basis $\langle \hat{\sigma}_B \rangle_w = 1$. Generalizing the QCC, we interpret this to mean that arm B has an elliptical polarization that is dependent on the phase difference between the interferometer arms.

A. Interpretation

The WV, defined relative to a given observable and a pair of pre- and postselected states [Eq. (3)], is formally unambiguous as it lies within the standard quantum-mechanical framework. It is the interpretation of the WV that is controversial. The reason for this is that traditionally quantum mechanics assigns properties to systems only upon projective measurements. Projective measurements, however, necessarily alter the quantum system's state; weak measurements seek to understand system properties in a nondestructive way.

Currently, interpretations of the WV can be categorized into three camps:

(1) WVs are numbers stemming from perturbation theory that have no relation to system properties [44].

(2) WVs are pre- and postselected ensemble averages (conditional expectation values) but do not represent *genuine* system properties [42].

(3) WVs partially represent local properties of the system for a given pair pre- and postselected in a retrodictive manner [45].

The QCC argument would fall in the third interpretative category. As such, we will adopt the interpretation that WVs do represent, at least partially, local properties of the system.

In the QCC it is implicitly assumed that $\langle \hat{\sigma}_A \rangle_w = 0$ corresponds to no polarization detected in arm A, which was not completely justified in the original paper. Let us review what occurs in a weak measurement. In a weak measurement, a measurement device weakly couples to the degree of freedom that one wishes to measure, e.g., a particle's polarization. After the interaction with the weak measurement device, one destructively measures the state of the system. If the final state of the system corresponds to some predefined postselected state, then one records the reading on the weak measurement device; otherwise, one ignores the reading.

Now if one wishes to interpret a reading on the measurement device as a measure of a property of the system, the interpretation of this value should be independent of the pre- and postselected states. Most notably, if one chooses the postselected state to be the same as the preselected state, then the WV is simply the expectation value, i.e., expectation values are a subset of weak values. The interpretation of the reading

on the measurement device should be consistent with the interpretation of the reading for the expectation value. Specifically, suppose we have a circular-polarization and a linear-polarization detector, $\hat{\sigma}_A^C$ and $\hat{\sigma}_A^L$. If $\langle \hat{\sigma}_A^C \rangle_w = \langle \psi_i | \hat{\sigma}_A^C | \psi_i \rangle_w = 1$ and -1 , this should be interpreted to mean that the particle is left- and right-circular polarized, respectively. Similarly, $\langle \hat{\sigma}_A^L \rangle_w = \langle \psi_i | \hat{\sigma}_A^L | \psi_i \rangle_w = 1$ and -1 should be interpreted to mean that the particle is horizontally and vertically polarized, respectively. Now, when $\langle \hat{\sigma}_A^C \rangle_w = 0$ this should be interpreted as no *circular* polarization, not necessarily no polarization, as claimed in the original QCC paper. The reason for this is illustrated when $|\psi_i\rangle = (|H\rangle + i|V\rangle)/\sqrt{2}$: here $\langle \hat{\sigma}_A^C \rangle_w = 0$ but $\langle \hat{\sigma}_A^L \rangle_w = 1$. In this case, the only consistent interpretation is that the particle is horizontally polarized. Building on this insight, we use the generalized QCC to complete the original QCC argument in a consistent manner.

Consider the case when $\phi - \theta = \pi/2$: $\langle \hat{\sigma}_A \rangle_w = 0$ and $\langle \hat{\sigma}_B \rangle_w = i$. For both operators, the WV is zero, as read by the expected value of the pointer, i.e., $\text{Re}\langle \hat{\sigma}_A \rangle_w = \text{Re}\langle \hat{\sigma}_B \rangle_w = 0$ (it is only the real component of WVs that shifts the pointer state [5]). Let us now rotate the basis of the polarization detector so that $\phi = \theta$: $\langle \hat{\sigma}_A \rangle_w = 0$ and $\langle \hat{\sigma}_B \rangle_w = 1$. Now in arm B, the measured WV is no longer 0; in comparison, the WV of polarization in arm A is still 0. In fact, it does not matter how we rotate the basis of the polarization operator, $\text{Re}\langle \hat{\sigma}_A \rangle_w$ will always be 0, whereas $\text{Re}\langle \hat{\sigma}_B \rangle_w = \cos(\phi - \theta)$ is in general nonzero.

Let us compare this with reading for the expectation value for a known polarized particle in arm B: $|\psi_i\rangle = (|H\rangle + e^{i\theta}|V\rangle)/\sqrt{2}$. The average reading on the measurement device is $\langle \hat{\sigma}_B \rangle = \cos(\phi - \theta')$, which exactly corresponds to the weak-value reading $\text{Re}\langle \hat{\sigma}_B \rangle_w$. In other words, a zero WV reading in the polarization pointer for arm B is polarization basis dependent, whereas for arm A the zero WV is basis independent. As $\langle \hat{\sigma}_A \rangle_w$ always vanishes no matter which polarization basis we measure, the generalized QCC supports the idea that $\langle \hat{\sigma}_A \rangle_w = 0$ should be interpreted as no polarization. This interpretation is also consistent with the expectation value, where there is no polarization only if $\langle \psi_i | \hat{\sigma}_A | \psi_i \rangle_w = 0 \forall \phi$; otherwise there is polarization.

There is another degree of freedom that we have not discussed, which is the choice of the spatial coordinate axes. Including this degree of freedom, the detector polarization basis is

$$|L\rangle \equiv (\cos \chi |H\rangle + e^{i\phi} \sin \chi |V\rangle)/\sqrt{2}, \quad (19)$$

$$|R\rangle \equiv (\sin \chi |H\rangle - e^{i\phi} \cos \chi |V\rangle)/\sqrt{2}, \quad (20)$$

where χ is the coordinate axes angle of rotation. This leads to

$$\langle \hat{\sigma}_A \rangle_w = 0, \quad (21)$$

$$\langle \hat{\sigma}_B \rangle_w = 2 \cos \chi \sin \chi e^{i(\phi-\theta)}. \quad (22)$$

For $\chi = 0$ or $\pi/2$, $\langle \hat{\sigma}_B \rangle_w = 0$. To determine whether this zero value is an artefact of the coordinate choice, one should rotate the coordinate axes of the polarization detectors. Note that to vary χ one can simply rotate the birefringent crystal that implements the polarization detector, whereas to vary ϕ one would need a different crystal with different refractive

properties (Sec. III C). If $\langle \hat{\sigma}_B \rangle_w$ is no longer zero after rotating the polarization detector, then one should attribute the zero reading to the choice of coordinate. This is consistent with the expectation value, which in arbitrary coordinate rotation is $\langle \psi_i | \hat{\sigma}_B | \psi_i \rangle_w = 2 \cos \chi \sin \chi \cos(\phi - \theta')$. For the rest of this paper, we will use coordinates where $\chi = \pi/4$.

B. Probability of detection

If there is no polarization in arm A, then a polarization detector should not interact with the system and therefore does not disturb it in any way. In contrast, the detection of polarization would necessarily disturb the system, affecting the probability of detection. Without interaction the probability of detection is the overlap between the preselected and postselected states; projected onto pointer basis q this is

$$\mathcal{P} = |\langle \psi_f | \psi_i \rangle|^2 |\langle q | m_i \rangle|^2. \quad (23)$$

In general, the probability of detection after interaction with the detector is

$$\mathcal{P}_\epsilon = |\langle q | \langle \psi_f | \hat{U} | m_i \rangle | \psi_i \rangle|^2, \quad (24)$$

where $\hat{U} = \exp(-\frac{i}{\hbar} g \hat{O} \hat{P})$.

To first order in g this gives [46]

$$\frac{\mathcal{P}_\epsilon}{\mathcal{P}} - 1 = \frac{2g}{\hbar} (\text{Re} \langle \hat{O} \rangle_w \text{Im} \langle \hat{P} \rangle_w + \text{Im} \langle \hat{O} \rangle_w \text{Re} \langle \hat{P} \rangle_w), \quad (25)$$

where

$$\langle \hat{P} \rangle_w = \frac{\langle q | \hat{P} | m_i \rangle}{\langle q | m_i \rangle}. \quad (26)$$

$\langle \hat{P} \rangle_w$ is the momentum WV of the pointer, which is dependent on the choice of basis. In Sec. III C we give specific examples.

Consider again the case $\langle \hat{\sigma}_A \rangle_w = 0$ and $\langle \hat{\sigma}_B \rangle_w = i$. From Eq. (25), we see no disturbance in the probability of detection in $\langle \hat{\sigma}_A \rangle_w = 0$, $\mathcal{P}_\epsilon = \mathcal{P}$, whereas for $\langle \hat{\sigma}_B \rangle_w = i$, there is a change in the probability of detection given by

$$\frac{\mathcal{P}_\epsilon}{\mathcal{P}} - 1 = \frac{2g}{\hbar} \text{Re} \langle \hat{P} \rangle_w. \quad (27)$$

In other words, the $\hat{\sigma}_B$ operator disturbs the probability of detection by an amount proportional to the momentum WV of the pointer.

In fact, this is true no matter what elliptical basis we choose to measure the polarization in. As $\langle \hat{\sigma}_A \rangle_w = 0$ always vanishes, the probability of detection is indistinguishable from no measurement, whereas $\langle \hat{\sigma}_B \rangle_w = e^{i(\phi - \theta)}$ will always disturb the probability of detection (for $\langle \hat{P} \rangle_w \neq 0$). As $\hat{\sigma}_A$ does not disturb the probability of detection and does not shift the polarization pointer, we identify $\langle \hat{\sigma}_A \rangle_w = 0$ as corresponding to no polarization.

The interpretation that $\langle \hat{\sigma}_A \rangle_w = 0$ corresponds to no polarization rests on the epistemic assumptions that WVs correspond to physical properties of a system and that these values are consistent with standard expectation values. Therefore, our interpretation is only as valid as the strength of these assumptions, which belong to the wider interpretive issue of WVs in general. However, adopting these assumptions has allowed us to extend the analysis of the QCC in a consistent manner.

C. Implementation

As a *gedanken* experiment, the authors of the QCC considered an interferometer setup with a series of optical elements and detectors for postselection, as laid out in Fig. 1. Postselection is achieved with a half-wave plate (HWP), phase shifter (PS2), beam splitter (BS2), and polarizing beam splitter (PBS). The HWP flips polarization $|H\rangle \leftrightarrow |V\rangle$. PS2 shifts the phase by i . The PBS transmits horizontal polarization and reflects vertical polarization. Under this construction, states orthogonal to $|\Phi_f\rangle$ will not trigger detector C1 (they will trigger C2 or C3), and $|\Phi_f\rangle$ will trigger C1 with certainty. Postselection means that we will consider only measurements that coincide with the triggering of C1.

The \hat{A} detector could be implemented with a sheet of glass placed in arm A [position D1 in Fig. 1(a)], slightly tilted up to produce a small vertical displacement of the beam. The C1 detector could be a CCD camera to record the beam deflection. Detection of the deflection would indicate the photon went via arm A. Similarly, the \hat{B} detector could be implemented with a sheet of glass placed in arm B [position D2 in Fig. 1(a)], slightly tilted down to produce a small vertical displacement of the beam.

$\hat{\sigma}_A$ and $\hat{\sigma}_B$ could be implemented with a birefringent crystal producing a small polarization-dependent horizontal beam displacement [46]. The eigenstates of $\hat{\sigma}_A$ and $\hat{\sigma}_B$ are left-elliptical $|L\rangle$ and right-elliptical $|R\rangle$ states; so for these polarizations, the refractive properties of the birefringent crystal should be so that the beam deflects left and right, respectively. For other polarization, a linear superposition of these basis states, the birefringent crystal would deflect left and right with polarization-dependent probability.

For weak measurements, the system state should be minimally disturbed; this means that the deflections should be less than the characteristic cross-section width of the beam, so that it is uncertain whether an individual photon has been deflected or not. Because of this, the experiment needs run to over a large ensemble to get the average of a single property.

As a specific implementation example, let us consider when the interferometer beam is a Gaussian so that

$$\langle x | m_i \rangle = \left(\frac{1}{2\pi\sigma^2} \right)^{1/4} \exp\left(-\frac{x^2}{4\sigma^2} \right). \quad (28)$$

For real WVs, from Eq. (4) the final pointer state projected onto the position basis is

$$\langle x | m_f \rangle \approx \frac{e^{i\theta}}{2} \left(\frac{1}{2\pi\sigma^2} \right)^{1/4} \exp\left[-\frac{(x - g\langle \hat{O} \rangle_w)^2}{4\sigma^2} \right]. \quad (29)$$

In other words, the Gaussian beam maintains its profile, but the interaction with the projectors deflects it by an amount proportional to the WV.

For $\langle \hat{\sigma}_A \rangle_w = 0$ and $\langle \hat{\sigma}_B \rangle_w = i$ we see no deflection in the beam on average; however there will be a difference in the total probability of detection between the two cases. In the position basis

$$\langle \hat{P} \rangle_w = \frac{\langle x | \hat{P} | m_i \rangle}{\langle x | m_i \rangle} = -i\hbar \frac{\partial_x m_i(x)}{m_i(x)} = i\hbar \frac{x}{2\sigma^2}. \quad (30)$$

This means that $\text{Re} \langle \hat{P} \rangle_w = 0$, and from Eq. (25) we do not observe any disturbance in the probability of detection for

$\langle \hat{\sigma}_A \rangle_w = 0$ and $\langle \hat{\sigma}_B \rangle_w = i$. However, if we measure in the momentum basis, then

$$\langle \hat{P} \rangle_w = \frac{\langle P | \hat{P} | m_i \rangle}{\langle P | m_i \rangle} = \frac{pm_i(p)}{m_i(p)} = p. \quad (31)$$

This can be implemented with a Fourier lens, so that each pixel on the CCD corresponds to a transverse momentum (Fig. 1). Using Eq. (31) in Eq. (25), we see no disturbance in the probability of detection for $\langle \hat{\sigma}_A \rangle_w = 0$, but there is a disturbance in the probability of detection proportional to the transverse momentum of the Gaussian beam for $\langle \hat{\sigma}_B \rangle_w = i$, thereby further distinguishing between no polarization and polarization.

Two actual attempts of realizing the QCC have been conducted with neutron [2] and photonic [3] interferometry. Although these experiments claimed to have produced the results of the gedanken experiment, they have been criticized for not actually implementing the QCC, as they do not make weak measurements [4].

IV. DUAL OF THE QUANTUM CHESHIRE CAT

Let us consider what would happen if the role of polarization and location were reversed in the QCC, i.e., under the transformation

$$|A\rangle \leftrightarrow |H\rangle, \quad |B\rangle \leftrightarrow |V\rangle. \quad (32)$$

For consistency with Sec. III, we will also use θ to indicate the phase difference between the arms and ϕ the polarization phase. The postselection state is invariant under this transformation, but the preselection state changes to

$$|\Psi_i\rangle = (e^{i\phi}|H\rangle + |V\rangle)|A\rangle/\sqrt{2}. \quad (33)$$

The projectors corresponding to the transformation are

$$\hat{H} = |H\rangle\langle H|(|+\rangle\langle +| + |-\rangle\langle -|), \quad (34)$$

$$\hat{V} = |V\rangle\langle V|(|+\rangle\langle +| + |-\rangle\langle -|), \quad (35)$$

and

$$\hat{\sigma}_H = |H\rangle\langle H|(|+\rangle\langle +| - |-\rangle\langle -|), \quad (36)$$

$$\hat{\sigma}_V = |V\rangle\langle V|(|+\rangle\langle +| - |-\rangle\langle -|), \quad (37)$$

where

$$|+\rangle \equiv (|A\rangle + e^{i\theta}|B\rangle)/\sqrt{2}, \quad (38)$$

$$|-\rangle \equiv (|A\rangle - e^{i\theta}|B\rangle)/\sqrt{2}. \quad (39)$$

\hat{H} and \hat{V} detect whether the photon is horizontally or vertically polarized. $\hat{\sigma}_H$ detects the phase difference between the arms for horizontal polarization. The eigenvalues 1 and -1 correspond to eigenstates $|+, H\rangle$ and $|-, H\rangle$, respectively, whereas the eigenvalue 0 corresponds to the degenerate subspace spanned by eigenstates $|+, V\rangle$ and $|-, V\rangle$. $\hat{\sigma}_V$ is similarly defined.

Using Eq. (3), the WVs measured are

$$\langle \hat{H} \rangle_w = \langle \hat{H} \hat{P} \rangle_w + \langle \hat{H} \hat{m} \rangle_w = 1, \quad (40)$$

$$\langle \hat{V} \rangle_w = \langle \hat{V} \hat{P} \rangle_w + \langle \hat{V} \hat{m} \rangle_w = 0 \quad (41)$$

and

$$\langle \hat{\sigma}_H \rangle_w = \langle \hat{H} \hat{P} \rangle_w - \langle \hat{H} \hat{m} \rangle_w = 0, \quad (42)$$

$$\langle \hat{\sigma}_V \rangle_w = \langle \hat{V} \hat{P} \rangle_w - \langle \hat{V} \hat{m} \rangle_w = e^{i(\phi-\theta)}, \quad (43)$$

where

$$\hat{p} = |+\rangle\langle +|(|H\rangle\langle H| + |V\rangle\langle V|), \quad (44)$$

$$\hat{m} = |-\rangle\langle -|(|H\rangle\langle H| + |V\rangle\langle V|). \quad (45)$$

Note that $\langle \hat{H} \hat{P} \rangle_w = \langle \hat{H} \hat{m} \rangle_w = 1/2$ and $\langle \hat{V} \hat{P} \rangle_w = -\langle \hat{V} \hat{m} \rangle_w = e^{i(\phi-\theta)}/2$. In this dual to the QCC, the photons are detected to be horizontally polarized, but the phase difference between the two arms is vertically polarized. What is even more remarkable is that in the preselection state, there is no arm B. In other words, it is as if the detector is detecting interference between arm A and a phantom arm B! The detected phase difference between arm A and B is determined by the photon's polarization in the preselected state. Specifically, by rotating the basis of the phase operators so that $\theta = \phi$ in Eqs. (38) and (39), one gets $\langle \hat{\sigma}_V \rangle_w = 1$. Analogous to the QCC, this is interpreted to mean that we have detected a phase difference, in the vertically polarized component, between arm A and arm B.

Rewriting

$$\hat{\sigma}_V = |V\rangle\langle V|(e^{-i\theta}|A\rangle\langle B| + e^{i\theta}|B\rangle\langle A|), \quad (46)$$

we see that $\hat{\sigma}_V$ has the property of flipping $|A\rangle$ and $|B\rangle$ (similarly for $\hat{\sigma}_H$). It is this property that underlies the apparent paradoxical phantom arm effect. This is exactly analogous to the central role that

$$\hat{\sigma}_B = |B\rangle\langle B|(e^{-i\phi}|H\rangle\langle V| + e^{i\phi}|V\rangle\langle H|) \quad (47)$$

(and similarly for $\hat{\sigma}_A$) plays in the QCC.

A. Implementation

Underpinning the QCC were the circular-polarization $\hat{\sigma}_A$ and $\hat{\sigma}_B$ detectors. They were proposed to be implemented as optical elements which slightly deflect the beam left (right) for left- (right-) circular polarization from the axis of arm A or B. This slight deflection provides the means to read the weak values on the CCD camera. Upon interaction, the detectors turn horizontal polarization vertical and vice versa, as described by Eq. (47). However, for weak interactions, this occurs only for a small subset of photons. Likewise, $\hat{\sigma}_H$ and $\hat{\sigma}_V$ should cause a slight left (right) deflection when the beams are in (out-of) phase. For a small subset of photons, arm A turns into arm B, as described by Eq. (46). This can be achieved by placing a PBS at position D1 in Fig. 4. The unitary transformation for the $\hat{\sigma}_V$ detector (similarly for $\hat{\sigma}_H$) is [47]

$$\hat{U} = e^{i\gamma\hat{\sigma}_V}. \quad (48)$$

The PBS is transparent to horizontal polarization but partially reflects vertical polarization, with reflectivity $r_V = \sin^2 \gamma$ and transmissivity $t_V = 1 - r_V$.

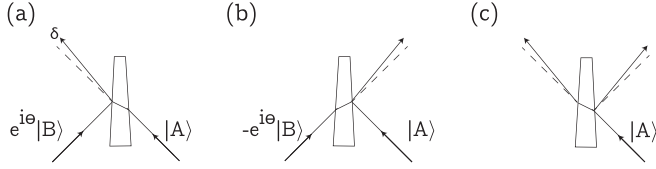


FIG. 2. $\hat{\sigma}_H$ ($\hat{\sigma}_V$) could be implemented with a wedged PBS. This figure illustrates Eqs. (55) and (56) for $\gamma = \pi/4$. The eigenstates of $\hat{\sigma}_H$ and $\hat{\sigma}_V$ are the $|+\rangle$ and $|-\rangle$ states; for such states the detector deflects the beam (a) left and (b) right, respectively. (c) For states composed of just one arm, the detector deflects left and right. The PBS is wedged so the deflection is slightly off the axis of the beam A or B (dotted lines). This small deflection δ provides the means to read the weak values on the CCD camera. For weak measurements, δ should not be greater than the cross-sectional width of the beam.

Considering just the vertical polarization component, we write $|A\rangle$ and $|B\rangle$ in terms of creation operators on the vacuum state $|0\rangle$:

$$|A\rangle = \hat{a}_A^\dagger |0\rangle, \quad |B\rangle = \hat{a}_B^\dagger |0\rangle. \quad (49)$$

In the Heisenberg picture, these operators transform under the PBSs as

$$\hat{U}^\dagger \begin{pmatrix} \hat{a}_A \\ \hat{a}_B \end{pmatrix} \hat{U} \equiv \begin{pmatrix} \hat{a}_{A'} \\ \hat{a}_{B'} \end{pmatrix}. \quad (50)$$

Using the Baker-Hausdorff lemma,

$$\hat{a}_{A'} = \hat{a}_A \cos \gamma + \hat{a}_B e^{-i\theta} \sin \gamma, \quad (51)$$

$$\hat{a}_{B'} = -\hat{a}_A e^{i\theta} \sin \gamma + \hat{a}_B \cos \gamma. \quad (52)$$

From Eqs. (51) and (52) we get

$$\hat{a}_A = \hat{a}_{A'} \cos \gamma - \hat{a}_{B'} e^{-i\theta} \sin \gamma, \quad (53)$$

$$\hat{a}_A \pm e^{-i\theta} \hat{a}_B = \hat{a}_{A'} (\cos \gamma \pm \sin \gamma) \pm \hat{a}_{B'} e^{-i\theta} (\cos \gamma \mp \sin \gamma). \quad (54)$$

Applying the conjugates of the operators in Eqs. (53) and (54) to the vacuum state, we see that the PBS transforms

$$|A\rangle \rightarrow \cos \gamma |A'\rangle - e^{-i\theta} \sin \gamma |B'\rangle, \quad (55)$$

$$|\pm\rangle \rightarrow [(\cos \gamma \pm \sin \gamma) |A'\rangle \pm e^{-i\theta} (\cos \gamma \mp \sin \gamma) |B'\rangle] / \sqrt{2}. \quad (56)$$

Equations (53)–(56) equally apply to the horizontal-polarization component for $\hat{\sigma}_H$.

Figure 2 illustrates Eqs. (55) and (56) for $\gamma = \pi/4$. The eigenstates of $\hat{\sigma}_H$ and $\hat{\sigma}_V$ are the $|+\rangle$ and $|-\rangle$ states, so for such states the detector deflects the beam left and right, respectively. For states composed of just one arm, the detector deflects left and right. The deflection should be slightly off the axis of beam A or B; as such the PBS should be slightly wedged. $\theta = 2\pi d/\lambda$ is the phase difference between the reflected and transmitted beams; it is determined by the path difference d due to the width of the PBS and wavelength λ . For weak interactions, γ should be small so that only a small subset of photons are deflected. Furthermore, the deflection δ should not be greater than the cross-sectional width of the beam.

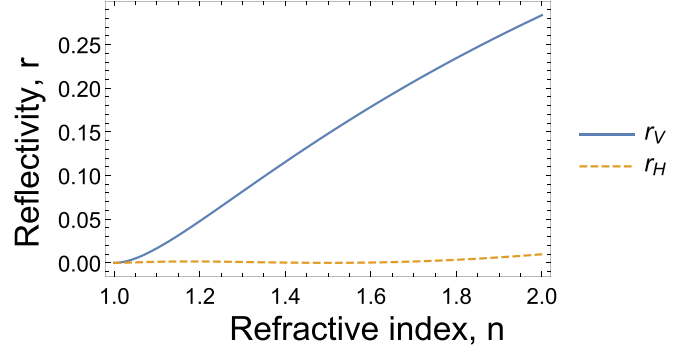


FIG. 3. A plot of reflectivity r_V and r_H for incident angle $v_i = \arctan(1.5) \approx 56^\circ$, for refractive indices between 1 and 2. For $n = 1.5$, $v_i = \arctan(1.5)$ is the Brewster angle with $r_H = 0$ and $r_V \approx 0.15$. This satisfies the requirement that $\hat{\sigma}_V$ transmits horizontal polarization but reflects vertical polarization with small probability.

The PBS can simply implemented as a piece of glass. The Fresnel reflections are different for the polarization component in the plane of incidence and the orthogonal component. We can define coordinates so that horizontal polarization is in the plane of incidence so that the reflectivities are

$$r_H = \left[\frac{\tan(v_i - v_t)}{\tan(v_i + v_t)} \right]^2, \quad r_V = \left[\frac{\sin(v_i - v_t)}{\sin(v_i + v_t)} \right]^2, \quad (57)$$

where v_i (v_t) is the angle of incidence (transmission).

$r_H = 0$ at the Brewster angle $v_i = \arctan(n)$, where $n \approx 1.5$ is the refractive index of glass. Figure 3 plots reflectivity as function of n , for $v_i = \arctan(1.5) \approx 56^\circ$. At the Brewster angle $r_V \approx 0.15$. This satisfies the requirement that $\hat{\sigma}_V$ transmits horizontal polarization but reflects vertical polarization with small probability. For $\hat{\sigma}_H$ one would orient the piece of glass (and experiment) so that the vertical-polarization component is in the plane of incidence.

\hat{H} and \hat{V} could be a birefringent crystal producing a small polarization-dependent horizontal beam displacement, placed at position D2 in Fig. 4. As with the QCC, the detectors only minimally disturb the beam and therefore can be measured simultaneously. In particular, measuring $\langle \hat{\sigma}_V \rangle_w$ and $\langle \hat{H} \rangle_w$ simultaneously will show that the phase difference is vertically polarized, but the photon is horizontally polarized. Note that to measure $\hat{\sigma}_V$ and $\hat{\sigma}_H$ simultaneously, one needs to duplicate the setup depicted in Fig. 4 for the two beams reflected by the detectors.

B. Temporal interference

At the heart of the QCC and its dual is the interplay between the preselected and postselected states; this gives rise to the concept of temporal interference in the QCC dual. To understand this idea, we compare it with a conventional notion of interference. In the double-slit experiment, every point on the detection screen can be considered as the interference between two light rays emanating from the slits. As rays from the two slits must travel different distances to different points on the screen, a phase differential arises. If we label the state of a photon emanating from slit α (β) as $|\alpha\rangle$ ($|\beta\rangle$), the interference is the result of the phase differential that arises from the spatial

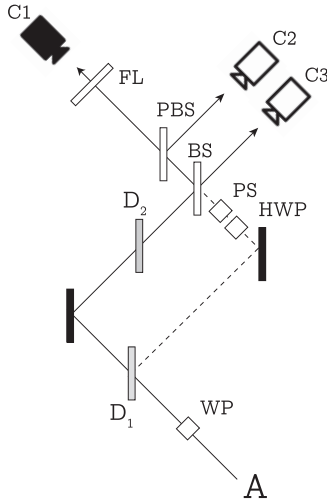


FIG. 4. A schematic of the phantom arm, where a wave plate (WP) introduces a controllable phase $e^{i\phi}$. A half-wave plate (HWP), phase shifter (PS), beam splitter (BS), and polarizing beam splitter (PBS) are used for postselection. To project the pointer onto the momentum basis, a Fourier lens (FL) is used to Fourier transform the light beam so that each pixel on the camera corresponds to a transverse momentum. To project the pointer onto the position basis, remove the FL, and each pixel corresponds to a transverse displacement. Detectors $\hat{\sigma}_H$ ($\hat{\sigma}_V$) are placed at location D_1 and \hat{H} (\hat{V}) at location D_2 . The solid line represents the axes of the main beam, and the dashed line represents the axes of the weak beam after interaction with the detector at position D_1 .

separation of $|\alpha\rangle$ and $|\beta\rangle$. $|\alpha\rangle$ is spatially separated from $|\beta\rangle$ in the sense that one is the spatial translation of the other.

The spatial separation of the slits is implemented in an interferometer with a controllable phase shift in one of the arms, as in $|\Phi_i\rangle$, where $|A\rangle$ and $|B\rangle$ would represent states of photons that went through slits α and β . In comparison, in $|\Psi_i\rangle$ there are no spatially separated states as there is just one arm of the interferometer (or equivalently, just one slit). In this case, the detected interference pattern arises from the phase differential between the preselected and postselected states; in other words, it is a temporal interference between past and future quantum states.

Reinforcing this notion, the preselection and postselection states themselves do not exhibit interference ($\hat{\sigma} = \hat{\sigma}_H$ or $\hat{\sigma}_V$): $\langle\Psi_i|\hat{\sigma}|\Psi_i\rangle = \langle\Psi_f|\hat{\sigma}|\Psi_f\rangle = 0$, whereas, in comparison $\langle\Psi_f|\hat{\sigma}|\Psi_i\rangle$ is in general nonzero. This is analogous to the fact that the $|\alpha\rangle$ and $|\beta\rangle$ do not exhibit interference on their own but rather arise from the phase difference between them.

The notion of WV temporal interference has been demonstrated with a driven superconducting qubit [48]. In this exper-

iment the fluorescence of qubits prepared in the ground and excited states were each measured. Then the fluorescence of the preselected excited state, postselected to be in the ground state was measured, and it showed a pattern which appeared to be the interference between the fluorescence of the previously measured ground- and excited-state patterns. The effect we propose here goes beyond this, as we propose that the interference is carried by horizontally polarized photons, yet the photons are detected to be vertically polarized.

We also point out that temporal uncertainty can give rise to frequency domain interference in systems with time-dependent amplitude modulation [49]. The dual of the QCC is distinctly different from this type of temporal interference, as the interference we describe is in the position domain and is the result of interference between past and future quantum states.

V. OUTLOOK

By generalizing the QCC with elliptical polarization, we showed that the WV of the polarization for the pre- and postselected states of the generalized QCC is determined by the phase difference in the interferometer. We also showed that the generalization provides a consistent way to interpret the zero WV of this polarization.

We explored the behavior of the position-polarization duality in the QCC. We have shown in the QCC dual that while the photons are horizontally polarized, their phases are vertically polarized. The QCC dual gives rise to temporal interference. The past and future states are particlelike, while the intermediate states are wavelike in that they exhibit interference.

In an experiment that directly addresses the question of the physical reality of observables before wave-function collapse, Kocsis *et al.* [35] used WVs to observe the individual trajectories of photons as they formed the interference pattern in the double-slit experiment. More recently, individual quantum trajectories of a superconducting circuit were also reconstructed using weak measurements [50]. As the interferometer setup in this work can map to the double-slit experiment, it would be interesting in future work to map the trajectories of individual photons along the lines of the Kocsis *et al.* experiment to see how the interference pattern arises as the photon evolves from the preselected to postselected state in the QCC dual. In addition, as the QCC has not been satisfactorily realized in experiments, the dual-QCC setup offers an alternative pathway to realization.

ACKNOWLEDGMENTS

The author thanks M. Lewenstein, M. Bera, A. Riera, and S. Quach for discussions and checking the manuscript. This work was financially supported by the Ramsay fellowship.

- [1] Y. Aharonov, S. Popescu, D. Rohrlich, and P. Skrzypczyk, Quantum cheshire cats, *New J. Phys.* **15**, 113015 (2013).
 [2] T. Denkmayr, H. Geppert, S. Sponar, H. Lemmel, A. Matzkin, J. Tollaksen, and Y. Hasegawa, Observation of a quantum

Cheshire cat in a matter-wave interferometer experiment, *Nat. Commun.* **5**, 4492 (2014).

- [3] J. M. Ashby, P. D. Schwarz, and M. Schlosshauer, Observation of the quantum paradox of separation of a single photon from one of its properties, *Phys. Rev. A* **94**, 012102 (2016).

- [4] Q. Duprey, S. Kanjilal, U. Sinha, D. Home, and A. Matzkin, The quantum Cheshire cat effect: Theoretical basis and observational implications, *Ann. Phys.* **391**, 1 (2018).
- [5] Y. Aharonov, D. Z. Albert, and L. Vaidman, How the Result of a Measurement of a Component of the Spin of a Spin-1/2 Particle Can Turn Out to Be 100, *Phys. Rev. Lett.* **60**, 1351 (1988).
- [6] Y. Aharonov and L. Vaidman, The two-state vector formalism of quantum mechanics, in *Time in Quantum Mechanics*, edited by J. G. Muga, R. Sala Mayato, and I. L. Egusquiza (Springer Berlin Heidelberg, 2002), pp. 369–412.
- [7] N. Brunner and C. Simon, Measuring Small Longitudinal Phase Shifts: Weak Measurements or Standard Interferometry? *Phys. Rev. Lett.* **105**, 010405 (2010).
- [8] P. B. Dixon, D. J. Starling, A. N. Jordan, and J. C. Howell, Ultrasensitive Beam Deflection Measurement via Interferometric Weak Value Amplification, *Phys. Rev. Lett.* **102**, 173601 (2009).
- [9] P. Egan and J. A. Stone, Weak-value thermostat with 0.2 mK precision, *Opt. Lett.* **37**, 4991 (2012).
- [10] A. Feizpour, X. Xing, and A. M. Steinberg, Amplifying Single-Photon Nonlinearity Using Weak Measurements, *Phys. Rev. Lett.* **107**, 133603 (2011).
- [11] J. M. Hogan, J. Hammer, S.-W. Chiow, S. Dickerson, D. M. S. Johnson, T. Kovachy, A. Sugarbaker, and M. A. Kasevich, Precision angle sensor using an optical lever inside a Sagnac interferometer, *Opt. Lett.* **36**, 1698 (2011).
- [12] O. Hosten and P. Kwiat, Observation of the spin Hall effect of light via weak measurements, *Science* **319**, 787 (2008).
- [13] G. Jayaswal, G. Mistura, and M. Merano, Observation of the Imbert-Fedorov effect via weak value amplification, *Opt. Lett.* **39**, 2266 (2014).
- [14] A. N. Jordan, J. Martínez-Rincón, and J. C. Howell, Technical Advantages for Weak-Value Amplification: When Less is More, *Phys. Rev. X* **4**, 011031 (2014).
- [15] G. C. Knee and E. M. Gauger, When Amplification with Weak Values Fails to Suppress Technical Noise, *Phys. Rev. X* **4**, 011032 (2014).
- [16] M. Pfeifer and P. Fischer, Weak value amplified optical activity measurements, *Opt. Express* **19**, 16508 (2011).
- [17] D. J. Starling, P. B. Dixon, A. N. Jordan, and J. C. Howell, Optimizing the signal-to-noise ratio of a beam-deflection measurement with interferometric weak values, *Phys. Rev. A* **80**, 041803(R) (2009).
- [18] D. J. Starling, P. B. Dixon, A. N. Jordan, and J. C. Howell, Precision frequency measurements with interferometric weak values, *Phys. Rev. A* **82**, 063822 (2010).
- [19] D. J. Starling, P. B. Dixon, N. S. Williams, A. N. Jordan, and J. C. Howell, Continuous phase amplification with a Sagnac interferometer, *Phys. Rev. A* **82**, 011802(R) (2010).
- [20] G. Strübi and C. Bruder, Measuring Ultrasmall Time Delays of Light by Joint Weak Measurements, *Phys. Rev. Lett.* **110**, 083605 (2013).
- [21] M. D. Turner, C. A. Hagedorn, S. Schlamminger, and J. H. Gundlach, Picoradian deflection measurement with an interferometric quasi-autocollimator using weak value amplification, *Opt. Lett.* **36**, 1479 (2011).
- [22] G. I. Visa, J. Martínez-Rincón, G. A. Howland, H. Frostig, I. Shomroni, B. Dayan, and J. C. Howell, Weak-values technique for velocity measurements, *Opt. Lett.* **38**, 2949 (2013).
- [23] X. Zhou, Z. Xiao, H. Luo, and S. Wen, Experimental observation of the spin Hall effect of light on a nanometal film via weak measurements, *Phys. Rev. A* **85**, 043809 (2012).
- [24] L. Zhou, Y. Turek, C. P. Sun, and F. Nori, Weak-value amplification of light deflection by a dark atomic ensemble, *Phys. Rev. A* **88**, 053815 (2013).
- [25] H. Kobayashi, S. Tamate, T. Nakanishi, K. Sugiyama, and M. Kitano, Direct observation of geometric phases using a three-pinhole interferometer, *Phys. Rev. A* **81**, 012104 (2010).
- [26] H. Kobayashi, S. Tamate, T. Nakanishi, K. Sugiyama, and M. Kitano, Observation of geometric phases in quantum erasers, *J. Phys. Soc. Jpn.* **80**, 034401 (2011).
- [27] J. S. Lundeen and A. M. Steinberg, Experimental Joint Weak Measurement on a Photon Pair as a Probe of Hardy’s Paradox, *Phys. Rev. Lett.* **102**, 020404 (2009).
- [28] J. S. Lundeen, B. Sutherland, A. Patel, C. Stewart, and C. Bamber, Direct measurement of the quantum wavefunction, *Nature*, **474**, 188 (2011).
- [29] C. Bamber and J. S. Lundeen, Observing Dirac’s Classical Phase Space Analog to the Quantum State, *Phys. Rev. Lett.* **112**, 070405 (2014).
- [30] M. Malik, M. P. J. Lavery, M. J. Padgett, R. W. Boyd, M. Mirhosseini, and J. Leach, Direct measurement of quantum state rotations, *Nat. Commun.* **5**, 3115 (2014).
- [31] J. Z. Salvail, M. Agnew, A. S. Johnson, E. Bolduc, J. Leach, and R. W. Boyd, Full characterization of polarization states of light via direct measurement, *Nat. Photonics* **7**, 316 (2013).
- [32] E. Sjöqvist, Geometric phase in weak measurements, *Phys. Lett. A* **359**, 187 (2006).
- [33] N. Brunner, V. Scarani, M. Wegmüller, M. Legré, and N. Gisin, Direct Measurement of Superluminal Group Velocity and Signal Velocity in an Optical Fiber, *Phys. Rev. Lett.* **93**, 203902 (2004).
- [34] R. Mir, J. S. Lundeen, M. W. Mitchell, A. M. Steinberg, J. L. Garretson, and H. M. Wiseman, A double-slit ‘which-way’ experiment on the complementarity-uncertainty debate, *New J. Phys.* **9**, 287 (2007).
- [35] S. Kocsis, B. Braverman, S. Ravets, M. J. Stevens, R. P. Mirin, L. K. Shalm, and A. M. Steinberg, Observing the average trajectories of single photons in a two-slit interferometer, *Science* **332**, 1170 (2011).
- [36] Y. Aharonov and A. Casher, Topological Quantum Effects for Neutral Particles, *Phys. Rev. Lett.* **53**, 319 (1984).
- [37] X.-G. He and B. H. J. McKellar, Topological phase due to electric dipole moment and magnetic monopole interaction, *Phys. Rev. A* **47**, 3424 (1993).
- [38] M. Wilkens, Quantum Phase of a Moving Dipole, *Phys. Rev. Lett.* **72**, 5 (1994).
- [39] Y. Aharonov and L. Vaidman, The two-state vector formalism: An updated review, in *Time in Quantum Mechanics*, edited by J. G. Muga, R. Sala Mayato, and Í. L. Egusquiza (Springer Berlin Heidelberg, 2008), pp. 399–447.
- [40] Y. Aharonov, S. Popescu, and J. Tollaksen, A time-symmetric formulation of quantum mechanics, *Phys. Today* **63**(11), 27 (2010).
- [41] S. Parrott, What do quantum “weak” measurements actually measure? [arXiv:0908.0035](https://arxiv.org/abs/0908.0035).

- [42] B. E. Y. Svensson, What is a quantum-mechanical “weak value” the value of? *Found. Phys.* **43**, 1193 (2013).
- [43] B. Svensson, Pedagogical review of quantum measurement theory with an emphasis on weak measurements, *Quanta* **2**, 18 (2013).
- [44] D. Sokolovski, The meaning of “anomalous weak values” in quantum and classical theories, *Phys. Lett. A* **379**, 1097 (2015).
- [45] A. Matzkin, Weak values and quantum properties, *Found. Phys.* **49**, 298 (2019).
- [46] J. Dressel, M. Malik, F. M. Miatto, A. N. Jordan, and R. W. Boyd, *Colloquium*: Understanding quantum weak values: Basics and applications, *Rev. Mod. Phys.* **86**, 307 (2014).
- [47] R. A. Campos, B. E. A. Saleh, and M. C. Teich, Quantum-mechanical lossless beam splitter: SU(2) symmetry and photon statistics, *Phys. Rev. A* **40**, 1371 (1989).
- [48] P. Campagne-Ibarcq, L. Bretheau, E. Flurin, A. Auffèves, F. Mallet, and B. Huard, Observing Interferences between Past and Future Quantum States in Resonance Fluorescence, *Phys. Rev. Lett.* **112**, 180402 (2014).
- [49] U. Hauser, W. Neuwirth, and N. Thesen, Time-dependent modulation of the probability amplitude of single photons, *Phys. Lett. A* **49**, 57 (1974).
- [50] S. J. Weber, A. Chantasri, J. Dressel, A. N. Jordan, K. W. Murch, and I. Siddiqi, Mapping the optimal route between two quantum states, *Nature (London)* **511**, 570 (2014).